

Electronic Supporting Information

Natural Abundance Oxygen-17 Solid-State NMR of Metal Organic Frameworks Enhanced by Dynamic Nuclear Polarization

Diego Carnevale,^{1,*} Georges Mouchaham,^{2,*} Sujing Wang,² Mathieu Baudin,^{1,3} Christian Serre,^{2,*}
Geoffrey Bodenhausen,¹ Daniel Abergel¹

¹ *Laboratoire des biomolécules, LBM, Département de chimie, École normale supérieure, PSL University, Sorbonne Université, CNRS, 75005 Paris, France*

² *Institut des Matériaux Poreux de Paris, Ecole Normale Supérieure, ESPCI Paris, CNRS, PSL University, 75005 Paris, France*

³ *Université de Paris, Laboratoire de Chimie et Biologie Pharmacologiques et Toxicologiques, CNRS UMR 8601, Université Paris Descartes, 45 rue des Saints Pères 75006 Paris France*

Corresponding authors: Diego Carnevale diego.carnevale@ens.psl.eu
Georges Mouchaham georges.mouchaham@ens.psl.eu
Christian Serre christian.serre@ens.psl.eu

Experimental details

NMR. The dry material was impregnated with a solution (“DNP juice”) of 13 mM AMUPOL in D₂O:H₂O = 90:10 (v:v) without any cryoprotectant and transferred to a 3.2 mm sapphire rotor. The CP spectra were recorded at $T = 100$ K in a $B_0 = 18.8$ T magnet (800.1 and 108.5 MHz for ¹H and ¹⁷O, respectively) coupled with a 527 GHz gyrotron and utilizing a spinning rate $\nu_R = 10$ kHz with a recycling delay of 1 s. The *rf*-field strength for the 90° ¹H pulse was 100 kHz and the contact time for the cross-polarization step was $\tau_c = 3$ ms, with *rf* field strengths of 65 and 26 kHz for ¹H and ¹⁷O, respectively. The spectra were referenced to adamantane and H₂O, for ¹H and ¹⁷O, respectively. Numerical simulations were performed with SIMPSON^[1] and employed 8×320 crystal orientations sampled with the REPULSION scheme.^[2]

DFT calculations. DFT calculations were performed utilizing Gaussian09.^[3] The structure of the Zr₁₂ cluster (**I**) shown in Fig. 1 was optimized with the B3LYP functional^[4,5] utilizing the Pople basis sets^[6] 3-21G (for ¹H and ¹³C), 6-311+G(d) (for ¹⁷O) and the LANL2DZ pseudopotential (for Zr).^[7-9] The optimized geometry was subsequently utilized for the calculation of magnetic shielding and EFG tensors with the GIAO method^[10,11] at the same level of theory. Subsequently, a single ¹H nucleus was positioned in the proximity of a μ_3 -O moiety. Geometry optimization allowed the position of this proton to be optimized, while the remaining structure was kept frozen. The resulting geometry was utilized for the calculations of NMR parameters as described above. Only the relevant μ_3 -O site was considered in this latter case. The EFGShield software^[12] was utilized to extract the calculated NMR parameters. Cartesian coordinates are given in Supplementary Information.

Materials and methods. All chemicals were purchased from commercial suppliers (ZrCl₄ and formic acid (Acros) and IPA (Alfa Aesar)) and used as received without further purification. Powder X-ray Diffraction (PXRD) patterns were recorded on a high-throughput Bruker D8 Advance diffractometer working on transmission mode and equipped with a focusing Göbel mirror producing CuK α radiation ($\lambda = 1.5418$ Å) and a LynxEye detector. N₂ gas sorption isotherms were measured on a Micromeritics® Tristar instrument at 77 K. Temperature was maintained using

liquid N₂ bath. Prior to the measurement, the MOF powder was heated at 120 °C under primary vacuum during 6 hours.

Synthesis of MIP-206. MIP-206 has been synthesized via solvothermal method following the procedure reported in reference [13] as described below:

Isophthalic acid (IPA; 1.1 g, 6.6 mmol) and formic acid (5 mL) were added into a 23 mL Teflon container and vigorously stirred at room temperature for 5 minutes until a homogeneous suspension was formed. ZrCl₄ (2 g, 8.6 mmol) was then added to the suspension followed by 10 minutes stirring at room temperature to disperse the reactants uniformly. The reaction was then sealed in an autoclave and heated to 180 °C in 2 hours and was kept at 180 °C for 24 hours. After cooling down to room temperature, the expected product of MIP-206 (1.98 g) was collected by filtration, washed with acetone and air dried.

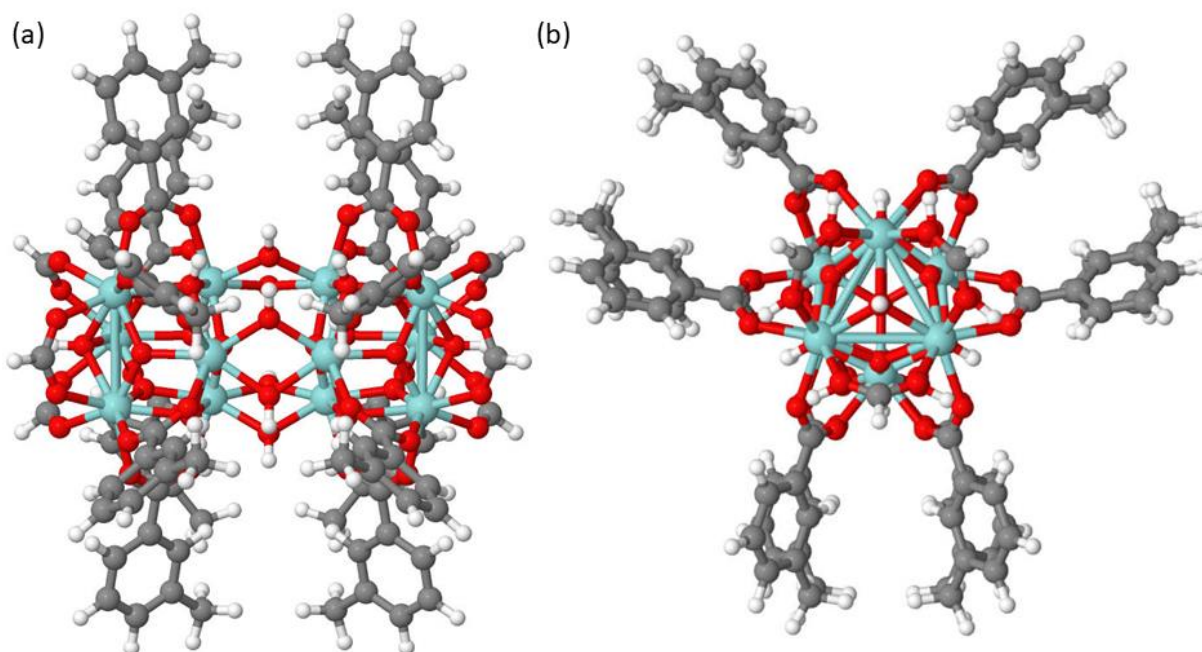


Figure S1. (a, b) Structure of the Zr₁₂ oxo-cluster (**I**) with the composition [Zr₁₂(μ₃-O)₈(μ₃-OH)₈(μ₂-OH)₆(HCOO)₆(L-COO)₁₂] (L-COO)₈ (where L stands for a 4 m-methylbenzene ring) comprising two subunits bridged by 6 protonated μ₂-O site units, viewed down the z- and x-axes, respectively. The Zr, C, O, H atoms are represented by blue-gray, grey, red and white spheres, respectively.

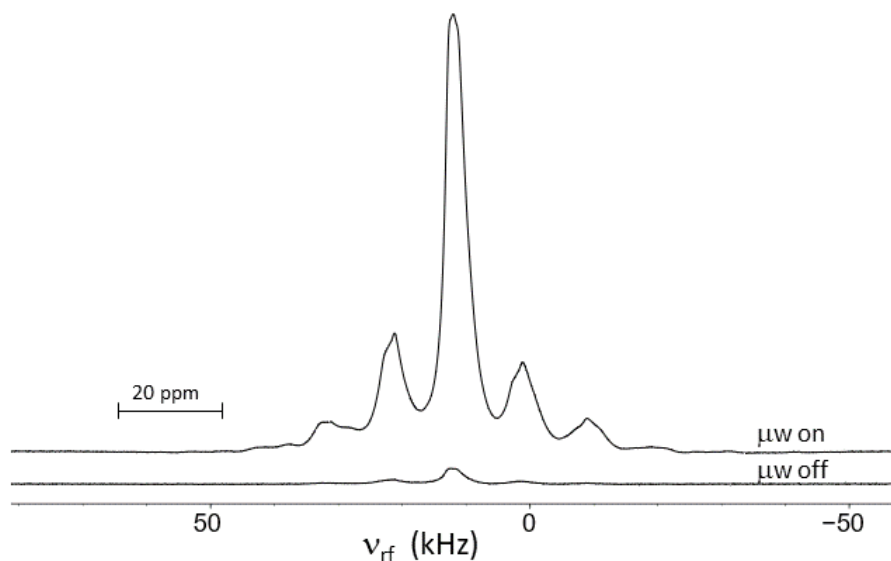


Figure S2. (a) Proton NMR spectra MIP-206, a porous polycrystalline MOF containing Zr₁₂ oxo-clusters (I) of the type shown in Fig. 1, acquired at 800 MHz with and without microwave irradiation, obtained by a solid echo ($90^\circ - \tau - 90^\circ - \tau -$ acquisition) on a sample of 30 mg with incipient wetness impregnation with an aqueous ($D_2O:H_2O = 90:10$) solution of 13 mM of the biradical AMUPOL as polarizing agent without cryoprotectant, observed at 100 K in a 3.2 mm sapphire rotor spinning about the magic angle at 10 kHz. The enhancement factor is $\epsilon(^1H) = S_{with}/S_{without} = 28$, allowing a saving in experimental time by a factor of ca. 800.

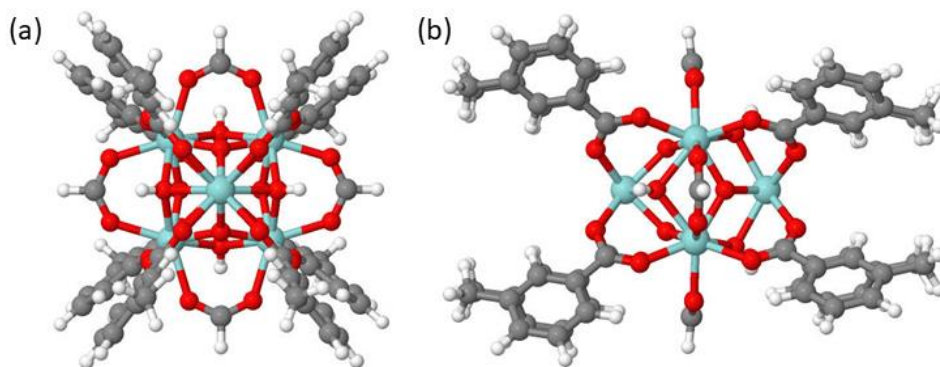


Figure S3. (a, b) Views of Zr₆-oxo-cluster (II) formulated $[Zr_6(\mu_3-O)_4(\mu_3-OH)_4(HCOO)_4(L-COO)_8]$ (where L stands for a 4 m-methylbenzene ring) showing that the core is similar to half of the Zr₁₂ cluster (I), but without the $(\mu_2-OH)_3$ bridges, viewed down the z- and x-axes, respectively.

Table S1 NMR parameters calculated by DFT for the Zr12 cluster (I) of Fig. 1.

Site	C_Q (MHz)	η_Q	δ_{iso}	Δ_{CS}	η_{CS}
$\mu 3\text{-OH}$	-8.18	0.01	17.00	51.66	0.29
	-8.18	0.01	17.54	50.86	0.25
	-8.18	0.01	17.77	51.18	0.25
	-8.07	0.00	1.32	82.67	0.01
$\mu 3\text{-O}$	1.07	0.01	412.11	101.31	0.03
	1.06	0.29	392.22	80.45	0.76
	1.06	0.28	390.94	83.10	0.75
	1.06	0.30	394.45	81.70	0.77
$\mu 3\text{-OH}^+$	-7.91	0.03	61.28	-10.35	0.31
$\mu 2\text{-OH}$	-8.77	0.51	135.29	-104.07	0.08
	-8.74	0.50	140.65	-107.80	0.02
	-8.77	0.51	137.56	-103.98	0.04
	-8.76	0.50	135.65	-102.38	0.05
	-8.78	0.51	133.09	-100.14	0.10
	-8.76	0.51	137.05	-105.28	0.06
ArCOO^-	7.77	0.92	263.65	224.28	0.48
	7.99	0.83	262.14	238.22	0.42
	7.77	0.92	264.38	224.47	0.48
	7.97	0.84	261.44	239.22	0.42
	7.74	0.93	261.91	225.43	0.49
	7.97	0.83	264.14	238.44	0.42
	7.74	0.92	264.83	222.77	0.50
	7.96	0.84	262.63	238.57	0.42
	7.75	0.92	263.62	225.57	0.49
	7.98	0.83	261.52	237.90	0.41
	7.77	0.92	263.56	221.78	0.49
	7.98	0.83	260.10	240.94	0.40
HCOO^-	7.95	0.73	301.22	234.21	0.73
	7.95	0.73	301.29	234.06	0.74
	7.94	0.73	301.51	233.96	0.74
	7.95	0.73	302.38	234.16	0.74
	7.94	0.73	301.15	234.51	0.74
	7.95	0.73	300.90	235.44	0.73
H_2O	6.70	0.94	-47.96	-28.56	0.73

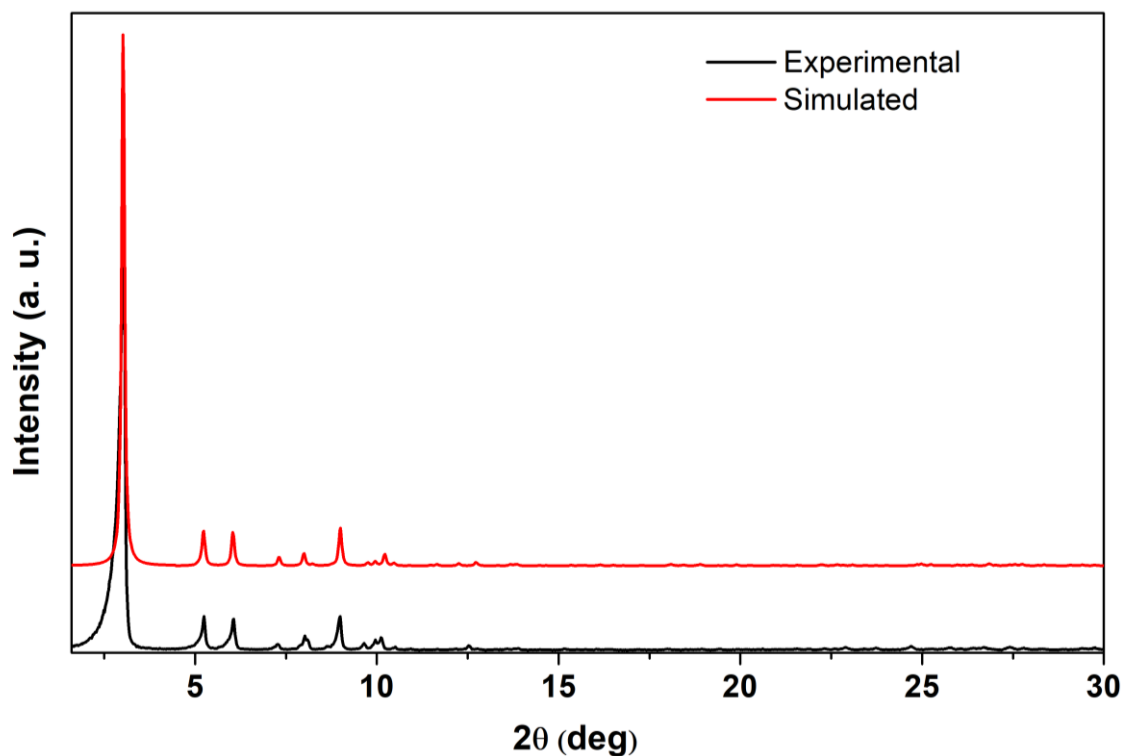


Figure S4. PXRD of MIP-206: Experimental vs simulated (obtained from DFT derived minimum energy structure) patterns.

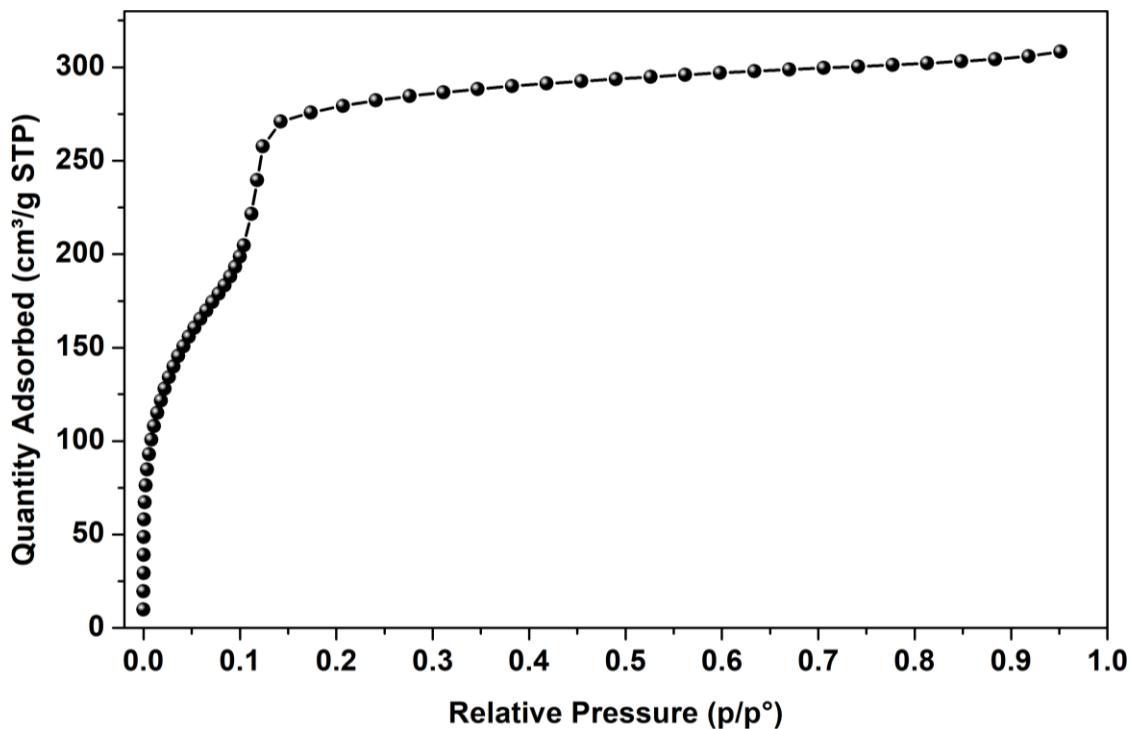


Figure S5. MIP-206 N_2 adsorption isotherm of measured at 77 K.

Cartesian coordinates of the Zr12 cluster of Figure 1.

O	-4.30070	1.92946	-3.45655
O	-4.27788	2.04965	3.40758
O	-4.29532	-3.96440	0.07389
O	4.28865	1.92371	-3.47566
O	4.30173	2.03560	3.38711
O	4.28239	-3.97238	0.05621
O	-4.28322	-2.89469	2.72091
O	-4.27961	3.80086	1.15390
O	-4.30029	-0.90400	-3.85088
O	4.28832	-2.90214	2.69931
O	4.29350	3.79157	1.13402
O	4.28047	-0.91058	-3.87314
O	6.48739	1.71172	-1.94188
O	6.49317	0.79787	2.43460
O	6.47931	-2.53757	-0.54507
O	6.48753	-1.45578	2.12022
O	6.48829	2.56766	0.16648
O	6.48095	-1.13724	-2.33841
O	-2.46197	2.99514	-2.68509
O	-2.45447	0.82439	3.94309
O	-2.46123	-3.82660	-1.24112
O	2.45575	2.99300	-2.69568
O	2.46897	0.82809	3.93067
O	2.45457	-3.82611	-1.26614
O	-2.45247	-1.87240	3.56801
O	-2.45410	4.02077	-0.16190
O	-2.47280	-2.15539	-3.39716
O	2.46696	-1.87267	3.55708
O	2.46079	4.01793	-0.17051
O	2.44355	-2.14817	-3.41755
C	-3.48124	2.90762	-3.44178
C	-3.45909	1.54376	4.24585

Natural abundance oxygen-17 solid-state NMR of metal organic frameworks enhanced by dynamic nuclear polarization

C	-3.47434	-4.44206	-0.77799
C	3.47317	2.90498	-3.45493
C	3.48275	1.53633	4.22923
C	3.46636	-4.44412	-0.80390
C	-3.45547	-2.65025	3.66057
C	-3.46209	4.48980	0.45746
C	-3.48703	-1.85429	-4.10419
C	3.47219	-2.64812	3.64663
C	3.47311	4.48379	0.44422
C	3.45473	-1.84894	-4.13000
C	-5.04127	-3.11281	-7.31610
C	-4.97883	7.91463	0.99034
C	-4.93554	-4.88519	6.33093
C	4.97512	-3.08294	-7.36706
C	4.99238	7.90480	0.99337
C	4.98076	-4.86342	6.31678
C	-5.01749	-7.86844	-1.21659
C	-4.96045	2.91155	7.43877
C	-5.07962	5.05885	-6.11327
C	5.01349	-7.86673	-1.25647
C	5.02034	2.88713	7.41163
C	5.06883	5.05183	-6.13124
C	-3.09189	-4.48545	-6.81217
C	-3.06185	8.14199	-0.49730
C	-3.03663	-3.69423	7.28689
C	3.03404	-4.46295	-6.85207
C	3.05994	8.14482	-0.47191
C	3.08440	-3.67528	7.28134
C	-3.05393	-7.71726	-2.65198
C	-3.03312	1.53693	8.01763
C	-3.10608	6.21276	-5.26930
C	3.04466	-7.71523	-2.68459
C	3.06622	1.55663	8.00278

C	3.08726	6.20019	-5.29869
C	-2.87355	-3.71494	-5.66395
C	-2.85061	6.76158	-0.40027
C	-2.83244	-3.07123	6.05010
C	2.82579	-3.70055	-5.69635
C	2.85144	6.76312	-0.38705
C	2.87093	-3.05587	6.04425
C	-2.84213	-6.41357	-2.18808
C	-2.83094	1.28626	6.65536
C	-2.87227	5.13666	-4.40653
C	2.83364	-6.41223	-2.21823
C	2.85688	1.30019	6.64248
C	2.85716	5.12804	-4.42985
C	-3.72980	-2.65524	-5.34332
C	-3.69527	5.96474	0.38144
C	-3.67394	-3.34700	4.96572
C	3.68380	-2.64160	-5.37725
C	3.70485	5.95946	0.37803
C	3.70511	-3.33381	4.95494
C	-3.70894	-5.84174	-1.24917
C	-3.68499	1.83942	5.69408
C	-3.73463	4.03336	-4.39261
C	3.70284	-5.84127	-1.28121
C	3.71956	1.83036	5.67609
C	3.72468	4.02898	-4.40837
C	-4.18285	-4.17064	-7.63333
C	-4.13259	8.70749	0.20836
C	-4.09456	-4.60480	7.41265
C	4.11566	-4.14041	-7.68232
C	4.13733	8.70450	0.22817
C	4.14552	-4.58262	7.40290
C	-4.14902	-8.43631	-2.15425
C	-4.10497	2.35666	8.39622

C	-4.21708	6.15898	-6.12312
C	4.14242	-8.43391	-2.19232
C	4.15545	2.35623	8.37414
C	4.20082	6.14760	-6.14906
C	-4.82139	-2.35207	-6.17060
C	-4.76739	6.54102	1.07849
C	-4.73300	-4.25578	5.10531
C	4.76615	-2.33106	-6.21378
C	4.78317	6.53018	1.07006
C	4.76800	-4.23897	5.09047
C	-4.80409	-6.56970	-0.76146
C	-4.75752	2.65426	6.08523
C	-4.84536	3.99280	-5.24722
C	4.80006	-6.56931	-0.79794
C	4.80884	2.62631	6.06014
C	4.83730	3.98902	-5.26059
H	5.80673	-2.85097	-8.02238
H	5.82020	8.35781	1.52659
H	5.79739	-5.56662	6.43267
H	5.85699	-8.43979	-0.88913
H	5.85781	3.50197	7.72053
H	5.92446	5.03079	-6.79629
H	-2.04133	-3.92894	-5.00147
H	-2.03441	6.28545	-0.93333
H	-2.02437	-2.36024	5.91287
H	2.00046	-3.92019	-5.02711
H	2.02964	6.29167	-0.91566
H	2.06106	-2.34627	5.91061
H	-2.00688	-5.82334	-2.55033
H	-2.01341	0.65576	6.32156
H	-2.02493	5.14156	-3.72893
H	1.99568	-5.82292	-2.57566
H	2.02510	0.68563	6.31442

H	2.00743	5.13183	-3.75528
H	-4.36218	-4.75985	-8.52654
H	-4.30570	9.77656	0.14308
H	-4.26218	-5.09531	8.36570
H	4.28715	-4.72349	-8.58108
H	4.30825	9.77446	0.17239
H	4.32085	-5.06967	8.35635
H	-4.32331	-9.44795	-2.50539
H	-4.27255	2.55894	9.44887
H	-4.40753	6.98643	-6.79852
H	4.31648	-9.44496	-2.54526
H	4.32832	2.56279	9.42515
H	4.38830	6.97193	-6.82909
H	5.42042	-1.51079	-5.94458
H	5.43403	5.88847	1.65149
H	5.40482	-4.43424	4.23624
H	5.46225	-6.10604	-0.07660
H	5.46648	3.02218	5.29580
H	5.49718	3.13069	-5.22469
Zr	-1.80388	-0.28896	2.08144
Zr	-1.81235	-1.65645	-1.28624
Zr	-1.80733	1.94220	-0.78893
Zr	1.81172	-0.29139	2.07218
Zr	1.80214	-1.65737	-1.29723
Zr	1.80754	1.94012	-0.79725
O	-2.41192	0.31899	-2.30038
O	-2.39924	1.83473	1.43205
O	-2.40536	-2.15443	0.87906
O	2.40153	0.31702	-2.31244
O	2.41002	1.83037	1.42039
O	2.40365	-2.15828	0.86589
Zr	-4.72923	1.62605	1.27341
Zr	-4.73470	-1.90395	0.78343

Zr	-4.73995	0.28573	-2.02774
Zr	4.73893	1.61662	1.25038
Zr	4.73230	-1.91319	0.75973
Zr	4.73092	0.27729	-2.05094
O	-3.89483	-1.35572	-1.04874
O	-3.89100	1.59607	-0.63989
O	-3.88795	-0.23456	1.71122
O	3.88639	-1.36221	-1.06903
O	3.89133	1.58920	-0.65865
O	3.89431	-0.24229	1.69233
H	2.15827	2.56788	1.99161
H	2.15002	-3.02218	1.21660
H	2.14038	0.44551	-3.23376
H	-2.14477	2.57265	2.00154
H	-2.14783	-3.01802	1.22760
H	-2.15693	0.44534	-3.22374
H	7.71389	-2.71459	-2.12545
H	7.72538	3.16607	-1.30474
H	7.72906	-0.48490	3.37287
O	5.73553	-0.00801	-0.01638
O	-1.46384	-0.00094	0.00120
O	1.46249	-0.00249	-0.00662
H	6.70221	-0.00973	-0.01811
O	0.00290	2.75807	0.15785
O	0.00405	-1.51993	2.30953
O	-0.00914	-1.23980	-2.47179
O	0.00602	0.82801	2.63187
O	-0.00276	1.85925	-2.04289
O	-0.00258	-2.69773	-0.59865
C	6.90146	2.49023	-1.03027
C	6.90423	-0.38210	2.65174
C	6.89257	-2.13688	-1.67532
H	-0.00574	1.88620	-3.00686

H	0.00845	1.68340	3.07666
H	-0.00275	-3.53955	-0.12823
H	0.00457	-2.43975	2.59954
H	0.00478	3.48605	0.79068
H	-0.01027	-1.02144	-3.41114
H	-5.88044	-2.88723	-7.96398
H	-5.80188	8.37207	1.52715
H	-5.74887	-5.59171	6.44965
H	-5.85944	-8.44147	-0.84571
H	-5.78446	3.54159	7.75319
H	-5.93375	5.03723	-6.78023
H	-5.47403	-1.53084	-5.90040
H	-5.41173	5.90439	1.67260
H	-5.37620	-4.44859	4.25531
H	-5.46560	-6.10492	-0.04050
H	-5.40933	3.06735	5.32498
H	-5.50166	3.13154	-5.21706
O	-6.47805	0.81241	2.46621
O	-6.48116	2.58125	0.19689
O	-5.73608	0.00341	0.01128
O	-6.48069	-1.44124	2.15273
O	-6.49043	-2.52399	-0.51199
O	-6.49521	-1.12465	-2.30617
O	-6.49196	1.72503	-1.91132
C	-6.89121	-0.36629	2.68638
C	-6.89986	2.50477	-0.99800
H	-6.70277	0.00477	0.01378
C	-6.90726	-2.12253	-1.64061
H	-7.71191	-0.46645	3.41250
H	-7.72297	3.18302	-1.26895
H	-7.73254	-2.69769	-2.08679
C	-2.12082	-8.32433	-3.68480
H	-2.14684	-7.74339	-4.61488

Natural abundance oxygen-17 solid-state NMR of metal organic frameworks enhanced by dynamic nuclear polarization

H	-1.08549	-8.32968	-3.32413
H	-2.40764	-9.35417	-3.91783
C	2.11102	-5.62296	-7.18097
H	2.14329	-6.37755	-6.38580
H	1.07301	-5.28318	-7.27665
H	2.40185	-6.10402	-8.11972
C	2.10487	-8.32249	-3.71118
H	2.12403	-7.74137	-4.64100
H	2.39062	-9.35224	-3.94625
H	1.07214	-8.32856	-3.34290
C	2.16245	7.40434	-5.29469
H	1.11439	7.09664	-5.38035
H	2.26962	7.96482	-4.35723
H	2.39106	8.08052	-6.12402
C	2.14293	9.00771	-1.32085
H	2.39542	10.06764	-1.22043
H	2.22964	8.73431	-2.37960
H	1.09517	8.87522	-1.02683
C	2.13332	0.96682	9.04598
H	1.10139	1.30082	8.88320
H	2.14145	-0.12858	8.99489
H	2.43388	1.26318	10.05542
C	2.18682	-3.35381	8.46309
H	2.49166	-3.91328	9.35262
H	2.23036	-2.28400	8.69957
H	1.14229	-3.60386	8.24204
C	-2.16757	-5.64349	-7.14421
H	-2.19592	-6.39840	-6.34924
H	-2.46025	-6.12450	-8.08241
H	-1.13040	-5.30156	-7.24304
C	-2.19048	7.42394	-5.25296
H	-2.31686	7.98541	-4.31836
H	-1.13890	7.12422	-5.32140

H	-2.41120	8.09682	-6.08709
C	-2.15561	8.99681	-1.36587
H	-2.25456	8.71310	-2.42090
H	-2.40740	10.05757	-1.27271
H	-1.10437	8.86758	-1.08304
C	-2.11085	0.91985	9.05446
H	-2.13925	-0.17459	8.99212
H	-1.07306	1.23651	8.89438
H	-2.40564	1.21189	10.06690
C	-2.13319	-3.37304	8.46432
H	-2.18389	-2.30490	8.70784
H	-2.42727	-3.94040	9.35251
H	-1.08837	-3.61311	8.23455

Cartesian coordinates of the Zr₆ cluster of Figure 3.

Zr	-2.52837	0.00076	-0.00762
Zr	0.00318	-1.78581	-1.79918
Zr	0.00076	1.78202	1.79296
Zr	-0.00299	-1.79781	1.78094
Zr	0.00699	1.79411	-1.78709
O	-3.58258	-1.35560	1.42915
O	-3.57478	1.35991	-1.44709
O	-3.57764	-1.34755	-1.45532
O	-3.57993	1.35114	1.43659
O	-1.04282	-0.00568	1.47169
O	-1.03741	0.00415	-1.48125
O	-1.40884	2.00793	0.00122
O	-1.41319	-2.00864	-0.01209
O	-1.97079	-2.46934	-2.59170
O	1.97739	-2.57690	-2.48208
O	-0.05804	-1.12660	-3.95930
O	0.06432	-3.95148	-1.15422
Zr	2.53243	-0.00463	0.00121

O	1.41805	0.00336	-2.01109
O	1.04287	-1.48085	-0.00622
O	-1.97454	2.46953	2.57890
O	1.97424	2.56886	2.48271
O	-0.06903	1.12310	3.95309
O	0.06836	3.94762	1.14846
O	1.41102	-0.00997	2.00981
O	1.04620	1.47500	0.00363
O	-1.97971	-2.48654	2.56249
O	1.96887	-2.59308	2.46537
O	-0.07153	-1.15316	3.94554
O	0.06019	-3.95892	1.12188
O	-1.96565	2.48707	-2.57504
O	1.98277	2.58540	-2.46490
O	-0.05563	1.14969	-3.95174
O	0.07248	3.95522	-1.12762
C	-3.19122	-2.15004	2.34831
C	-3.17872	2.15375	-2.36474
C	-3.18318	-2.13501	-2.37913
C	-3.18695	2.13865	2.36099
H	-1.97979	2.78869	0.00334
H	-1.98570	-2.78827	-0.01520
C	3.18857	-2.36863	-2.14035
C	-0.12657	0.01342	-4.51146
C	0.13234	-4.51120	-0.01783
O	3.57988	1.43203	1.36006
O	3.58133	-1.44352	-1.35399
O	3.58462	1.44010	-1.34551
O	3.57675	-1.45128	1.35147
H	1.99357	0.00554	-2.78832
C	3.18633	2.35667	2.14662
C	-0.14191	-0.01677	4.50504
C	0.14163	4.50729	0.01236

Natural abundance oxygen-17 solid-state NMR of metal organic frameworks enhanced by dynamic nuclear polarization

H	1.98377	-0.01290	2.78908
C	3.18133	-2.38180	2.13005
C	3.19377	2.37047	-2.12664
H	-0.24835	0.01728	-5.60482
H	0.25410	-5.60458	-0.02128
H	-0.26757	-0.02036	5.59795
H	0.26568	5.60040	0.01634
C	-4.23734	-2.74540	3.23421
C	-4.22224	2.76495	-3.24289
C	-4.22831	-2.74274	-3.25780
C	-4.23220	2.73274	3.24885
C	4.23060	-3.26709	-2.72376
C	4.22681	3.26065	2.72435
C	4.22200	-3.27984	2.71676
C	4.23673	3.27524	-2.69864
C	-5.58694	-2.42402	3.03285
C	-3.86529	-3.61968	4.26318
C	-5.57444	2.45626	-3.03773
C	-3.84584	3.64423	-4.26572
C	-5.58102	-2.44536	-3.04065
C	-3.85268	-3.60821	-4.29283
C	-5.58400	2.42845	3.03498
C	-3.85764	3.59155	4.28965
C	3.85258	-4.31245	-3.57531
C	5.58157	-3.06584	-2.40747
C	3.84727	4.30810	3.57269
C	5.57766	3.06276	2.40560
C	3.84075	-4.33270	3.55757
C	5.57514	-3.06885	2.41664
C	3.85954	4.33293	-3.53522
C	5.58782	3.06662	-2.38774
C	-6.57865	-2.96952	3.85217
H	-5.84513	-1.74538	2.22736

C	-4.85037	-4.16900	5.08297
H	-2.81736	-3.85465	4.40166
C	-6.56401	3.01976	-3.84702
H	-5.83601	1.77351	-2.23688
C	-4.82895	4.21094	-5.07634
H	-2.79617	3.86968	-4.40699
C	-6.57217	-3.00671	-3.84972
H	-5.84202	-1.77419	-2.22986
C	-4.83714	-4.17182	-5.10377
H	-2.80247	-3.82504	-4.44324
C	-6.57519	2.97709	3.85256
H	-5.84419	1.76224	2.21987
C	-4.84222	4.14256	5.10918
H	-2.80818	3.81352	4.43770
H	2.80354	-4.45208	-3.80483
C	4.83277	-5.15081	-4.10572
C	6.56846	-3.90060	-2.93722
H	5.84415	-2.25064	-1.74316
H	2.79829	4.44516	3.80399
C	4.82594	5.15148	4.09789
C	6.56306	3.90267	2.93001
H	5.84144	2.24604	1.74364
H	2.79008	-4.47975	3.77471
C	4.81988	-5.16888	4.09335
C	6.56107	-3.90075	2.95269
H	5.84037	-2.24742	1.76114
H	2.81039	4.47811	-3.76067
C	4.84070	5.17607	-4.05617
C	6.57577	3.90547	-2.90894
H	5.84987	2.24147	-1.73561
H	-4.57383	-4.84861	5.88069
H	-4.54875	4.89443	-5.86946
H	-4.55764	-4.84431	-5.90649

H	-4.56350	4.81015	5.91625
H	4.55094	-5.96468	-4.76372
H	4.54303	5.96678	4.75364
H	4.53555	-5.98850	4.74310
H	4.55960	5.99940	-4.70261
C	8.04387	3.67898	-2.59157
H	8.58775	3.35210	-3.48641
H	8.51243	4.60116	-2.22943
H	8.16010	2.90929	-1.82264
C	-8.04090	-2.60884	3.65500
H	-8.67667	-3.49888	3.71750
H	-8.37085	-1.90223	4.42702
H	-8.19729	-2.14166	2.67772
C	-8.04084	2.64076	3.63832
H	-8.40385	1.97437	4.43084
H	-8.65694	3.54683	3.65001
H	-8.18703	2.13780	2.67742
C	-8.03869	-2.67566	-3.63309
H	-8.39882	-1.99195	-4.41212
H	-8.65453	-3.58122	-3.66703
H	-8.18848	-2.19365	-2.66204
C	8.03630	-3.68318	-2.61233
H	8.50138	-4.61231	-2.26377
H	8.58357	-3.34348	-3.50032
H	8.15248	-2.92628	-1.83081
C	8.03125	-3.67137	2.64720
H	8.56434	-3.32965	3.54301
H	8.50797	-4.59603	2.30250
H	8.15168	-2.91163	1.86908
C	-8.03007	2.67896	-3.64280
H	-8.64363	3.58654	-3.61650
H	-8.39704	2.04596	-4.46034
H	-8.17528	2.13852	-2.70234

C	8.03085	3.68850	2.60283
H	8.49323	4.61849	2.25299
H	8.58027	3.35059	3.49018
H	8.14754	2.93132	1.82164
C	6.17717	-4.94646	-3.78914
H	6.93413	-5.60476	-4.20375
C	-6.18361	-3.87458	-4.88288
C	-6.17462	3.90200	-4.86789
C	6.18532	4.96390	-3.74551
C	6.17032	4.95042	3.77883
C	6.16653	-4.95433	3.79351
C	-6.19385	-3.84717	4.87836
C	-6.18765	3.83872	4.89151
H	6.92277	-5.61045	4.21288
H	-6.95470	-4.28096	5.51951
H	-6.93392	4.34837	-5.50226
H	6.94270	5.62618	-4.15296
H	6.92565	5.61339	4.18894
H	-6.94394	-4.32028	-5.51644
H	-6.94822	4.27347	5.53241

References

- [1] M. Bak, J. T. Rasmussen, N. C. Nielsen, *J. Magn. Reson.* **2000**, *147*, 296–330.
- [2] M. Bak, N. C. Nielsen, *J. Magn. Reson.* **1997**, *125*, 132–139.
- [3] M. J. Frisch, G. W. Trucks, H. B. Schlegel, G. E. Scuseria, M. A. Robb, J. R. Cheeseman, G. Scalmani, V. Barone, B. Mennucci, G. A. Petersson, H. Nakatsuji, M. Caricato, X. Li, H. P. Hratchian, A. F. Izmaylov, J. Bloino, G. Zheng, J. L. Sonnenberg, M. Hada, M. Ehara, K. Toyota, R. Fukuda, J. Hasegawa, M. Ishida, T. Nakajima, Y. Honda, O. Kitao, H. Nakai, T. Vreven, J. Montgomery, J. A., J. E. Peralta, F. Ogliaro, M. Bearpark, J. J. Heyd, E. Brothers, K. N. Kudin, V. N. Staroverov, R. Kobayashi, J. Normand, K. Raghavachari, A. Rendell, J. C. Burant, S. S. Iyengar, J. Tomasi, M. Cossi, N. Rega, J. M. Millam, M. Klene, J. E. Knox, J. B. Cross, V. Bakken, C. Adamo, J. Jaramillo, R. Gomperts, R. E. Stratmann, O. Yazyev, A. J. Austin, R. Cammi, C. Pomelli, J. W. Ochterski, R. L. Martin, K. Morokuma, V. G. Zakrzewski, G. A. Voth, P. Salvador, J. J. Dannenberg, S. Dapprich, A. D. Daniels, Ö. Farkas, J. B. Foresman, J. V. Ortiz, J. Cioslowski and D. J. Fox, Gaussian, Inc., Wallingford CT, 2009.
- [4] A. D. Becke, *J. Chem. Phys.* **1993**, *98*, 5648–5652.
- [5] C. Lee, W. Yang, R. G. Parr, *Phys. Rev. B* **1988**, *37*, 785–789.
- [6] R. Ditchfield, W. J. Hehre, J. A. Pople, *J. Chem. Phys.* **1971**, *54*, 724–728.

- [7] P. J. Hay, W. R. Wadt, *J. Chem. Phys.* **1985**, *82*, 299–310.
- [8] W. R. Wadt, P. J. Hay, *J. Chem. Phys.* **1985**, *82*, 284–298.
- [9] P. J. Hay, W. R. Wadt, *J. Chem. Phys.* **1985**, *82*, 270–283.
- [10] D. Zeroka, H. F. Hameka, *J. Chem. Phys.* **1966**, *45*, 300–311.
- [11] R. Ditchfield, *J. Chem. Phys.* **1972**, *56*, 5688–5691.
- [12] S. Adiga, D. Aebi, D. L. Bryce, *Can. J. Chem.* **2007**, *85*, 496–505.
- [13] S. Wang, L. Chen, M. Wahiduzzaman, A. Tissot, L. Zhou, I. A. Ibarra, A. Gutiérrez-Alejandre, J. S. Lee, J.-S. Chang, Z. Liu, J. Marrot, W. Shepard, G. Maurin, Q. Xu, C. Serre. ChemRxiv. Preprint. <https://doi.org/10.26434/chemrxiv.12661310.v1>.